Eur Biophys J (1984) 11:95–102

European Biophysics Journal

An investigation into the solution structure of the single-stranded DNA undecamer 5′d AAGTGTGATAT by means of nuclear Overhauser enhancement measurements

G. M. Clore* and A. M. Gronenborn*

Division of Physical Biochemistry, National Institute for Medical Research, Mill Hill, London NW7 1AA, United Kingdom

Received March 5, 1984/Accepted May 24, 1984

Abstract. A 500-MHz ^{1}H-NMR study on the single-stranded DNA undecamer (11-mer) 5′d AAGTGTGATAT is presented. Using a combination of one-dimensional pre-steady-state nuclear Overhauser enhancement (NOE) measurements and two-dimensional homonuclear J-correlated spectroscopy, virtually complete resonance assignments are obtained. The relative magnitudes of the intra- and internucleotide NOEs indicate that the overall structure of the single-stranded 11-mer is a right-handed B-type helix with extensive base stacking. Within this overall structure there is quite a large degree of variability, as exemplified by variations in glycosidic bond and sugar pucker conformations, most likely determined by base sequence.

Key words: Single-stranded DNA, oligonucleotide, solution structure, NMR, nuclear Overhauser effect

Introduction

A variety of important cellular processes, such as DNA replication, recombination and repair, all require the presence of segments of single-stranded DNA. In most cases these are generated from double-stranded DNA by single-stranded DNA binding proteins and are intermediates for new double-stranded structures (see Meselson 1967; Radding 1978; McEntee et al. 1981; Kornberg 1980; Kowalczykoswki et al. 1981, for reviews). Thus the structural features of single-stranded DNA are of considerable biological interest. In contrast to double-stranded DNA where a wealth of fibre diffraction and more recently single-crystal data is available (see Arnott et al. 1983; Rich 1983; Dickerson et al. 1983; Viswamitra 1983; Wang et al. 1983, for reviews), the only crystallographic data available on single-stranded DNA is on the dimer dpTpT (Camerman et al. 1976).

Of the various physicochemical techniques available to study structure in solution, the nuclear Overhauser effect (NOE), as measured by NMR spectroscopy, is extremely powerful as it can be used to demonstrate the proximity of two protons in space and determine their separation (Noggle and Schirmer 1971; Redfield and Gupta 1971; Poulsen et al. 1980; Wagner et al. 1981; Wagner and Wüthrich 1982; Wider et al. 1982; Clore et al. 1984). Over the last year, the application of NOE measurements to double-stranded DNA oligonucleotides, up to 17 base pairs in length, has met with considerable success (Reid et al. 1983a, b; Clore and Gronenborn 1983, 1984; Gronenborn et al. 1983, 1984; Scheek et al. 1983; Hare et al. 1983; Weiss et al. 1984). However, there have been no extensive NOE studies on single-stranded DNA oligonucleotides. NMR studies on single-stranded DNA oligonucleotides have been limited to lengths of five bases or less (Cheng and Sarma 1977; Olsthoorn et al. 1980; Mellema et al. 1981; Neumann et al. 1982; Cheng et al. 1982; Altona 1982). In all these studies, assignment of resonances to individual residues was based on chemical shift arguments, temperature dependence of chemicals shifts and incremental procedures relying on numerous subfragments, and structural information was principally deduced from empirical Karplus (1963) type relationships, relating dihedral angles to three bond spin-spin coupling constants.

In this paper a NOE study on the single-stranded DNA undecamer (11-mer), 5′d AAGTGTGATAT, is presented. Using a combination of one-dimensional pre-steady state NOE measurements and two-dimensional homonuclear J-correlated spectros-

Abbreviations: NOE, nuclear Overhauser effect; COSY, two-dimensional homonuclear J-correlated spectroscopy; 11-mer, undecamer; EDTA, sodium ethylenediamine tetraacetate; HPLC, high-pressure liquid chromatography; DSS, 4,4-dimethylsilapentane-1-sulfonate

* Present address: Max-Planck Institut für Biochemie, D-8033 Martinsried bei München, FRG

copy (COSY), virtually complete resonance assignments are obtained. From a qualitative interpretation of the NOE data it is deduced that the single-stranded 11-mer predominantly adopts a B-type right-handed helical conformation in solution.

Experimental

5′d AAGTGTGATAT was prepared from suitably protected nucleosides by the solid-state phosphotriester method and purified by ion exchange HPLC, using a Partisil 10 SAX column essentially as described by Gait et al. (1982). The sequence of the 11-mer was checked by DNA sequencing as described by Maxam and Gilbert (1980). After desalting and extensive lyophilisation, the 11-mer (final concentration 6 mM) was dissolved in 99.96% D_2O containing 500 mM KCl, 50 mM potassium phosphate pH* 6.8 (meter reading uncorrected for the isotope effect on the glass electrode) and 0.1 mM EDTA.

All NMR spectra were recorded on a Bruker AM500 spectrometer operating in Fourier transform mode with quadrature detection. NOE spectra were recorded with a 90° observation pulse (pulse length 9 μs), an acquisition time of 0.5 s (8K data points and an 8.2-KHz spectral width) and a relaxation delay of 2 s. The NOEs were observed by directly collecting the difference free induction decay by interleaving eight transients after saturation for 1 s of a given resonance, with eight transients of off-resonance irradiation applied for the same length of time. $J_{1'2'}$ coupling constants were measured from a spectrum obtained with 64K data points for a 5.0-KHz spectral width (0.15 Hz/point resolution). The two-dimensional COSY spectrum was recorded with a sequence of two non-selective 90° pulses (Aue et al. 1976;

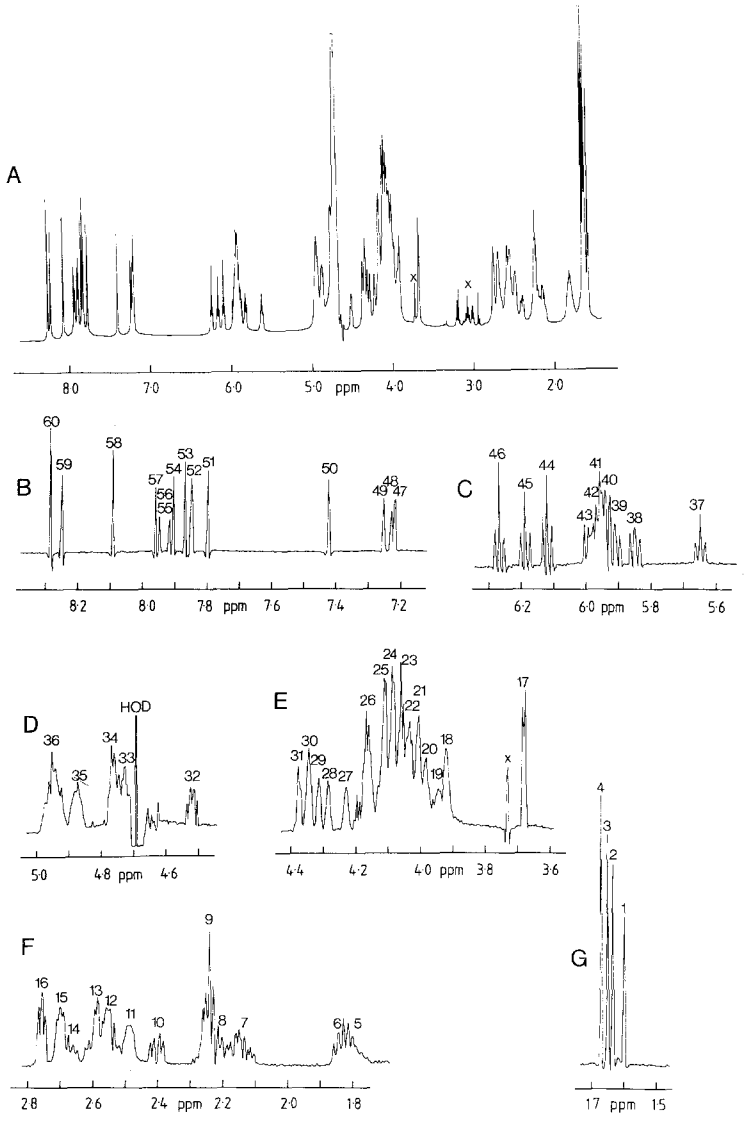

Fig. 1A–G. 500 MHz ^{1}H-NMR spectrum of the single-stranded DNA 11-mer in 99.96% D_2O at 30° C. **A** Complete spectrum between 1.5 and 8.5 ppm. **B, C, D, E, F,** and **G,** resolution enhanced expansions of the H8/H6/H2 (7.2–8.3 ppm), H1′ (5.6–6.3 ppm), H3′ (4.5–5.0 ppm), H4′/H5′/H5″ (3.6–4.4 ppm), H2′/H2″ (1.7–2.8 ppm), and CH_3 (1.5–1.7 ppm) regions respectively. The assignments of the numbered resonances are given in Table 1. Experimental conditions: 6 mM single-stranded 11-mer in 99.96% D_2O containing 500 mM KCl, 50 mM potassium phosphate pH* 6.8 and 0.1 mM EDTA; temperature, 30° C. The peaks marked *x* arise from low-molecular-weight impurities. The expansions were resolution enhanced by multiplying the free induction decay by a two-term exponential function (Lorentz-Gauss multiplication) prior to Fourier transformation

Wider et al. 1984): 90°-t_1-90°-t_2. 1K data points were sampled over a sweep width of 3,676 Hz in t_2, and 256 t_1 values were obtained with 64 transients for each t_1 value. The time domain matrix was appropriately zero-filled to end up with a 1K × 1K data matrix in the frequency domain (corresponding to a spectral resolution of 3.59 Hz/point) and prior to Fourier transformation, the time domain matrix was multiplied by a sine bell in both t_1 and t_2 directions. After Fourier transformation the spectrum was further improved by symmetrization (Baumann et al. 1981). The final COSY spectrum is shown as a contour plot in the absolute value (i.e., magnitude spectrum) presentation. Chemical shifts are expressed relative to 4,4-dimethylsilapentane-1-sulfonate (DSS). All experiments were carried out at 30° C.

Results and discussion

Sequential resonance assignment

Figure 1 shows the 500 MHz ^{1}H-NMR spectrum of 5'd AAGTGTGATAT in 99.96% D_2O containing 500 mM KCl at 30° C. The two-dimensional COSY spectrum is shown in Fig. 2 and permits the grouping of sugar resonance to spin systems along the intranucleotide pathway H1'→H2'/H2''→H3'→H4'→H5'/H5''. The chemical shift dispersion of the H3' resonances is limited so that the intranucleotide connectivity from the H3' to the H4' resonance cannot be established unambiguously from the COSY spectrum alone. This problem can, however, be overcome by making use of NOE measurements (see below) to connect the H1' and H4' protons of the same residue on the basis of their close spatial proximity (< 4 Å). In addition, the connectivity between the H6 and methyl protons of the T residues via their four bond spin-spin coupling is readily observed in the COSY spectrum.

To assign resonances to protons of particular residues we have made use of one-dimensional pre-steady state NOE measurements (Wagner and Wüthrich 1979; Dobson et al. 1982). These experiments were carried out under conditions where the magnitude of the NOE, N_{ij}, observed between the resonances of protons i and j, is proportional to the cross-relaxation rate σ_{ij} and hence to the reciprocal of the sixth power of the distance r_{ij}^{-6} between these two protons. Under such conditions NOEs are only detectable up to distances of ~ 5 Å, beyond which the effects fall to less than −1% and become virtually unobservable, thereby enabling NOE sequential resonance assignment strategies to be devised on the basis of the known structures of right-handed DNA (Reid et al. 1983a; Clore and Gronenborn 1983, 1984; Scheek et al. 1983; Gronenborn et al. 1984). Figure 3 summarizes a comprehensive NOE strategy for the

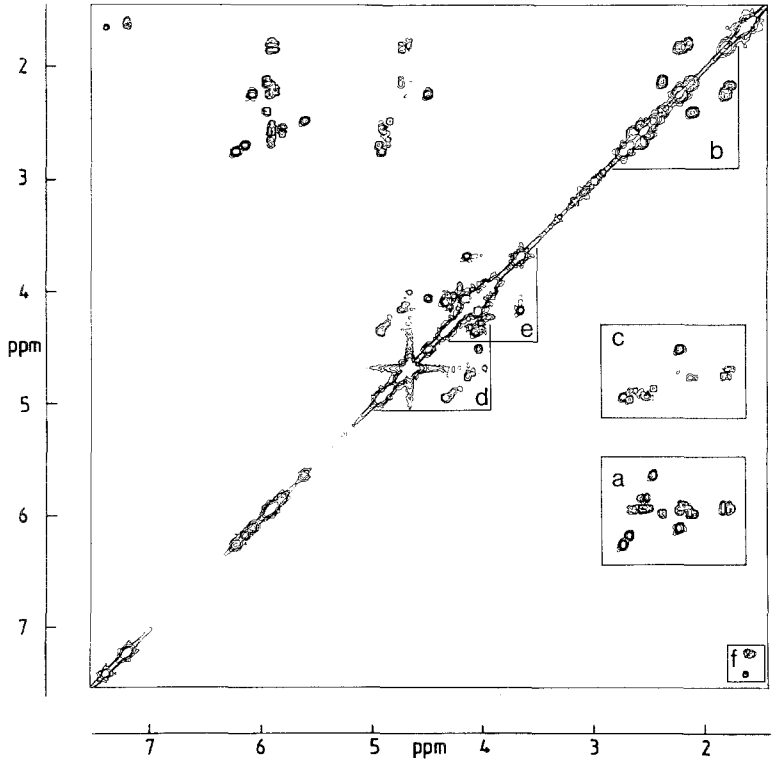

Fig. 2. 500 MHz COSY spectrum of the single-stranded DNA 11-mer between 1.5 and 7.5 ppm. The cross-peaks corresponding to the H1' ↔ H2'/H2'', H2' ↔ H2'', H2'/H2'' ↔ H3', H3' ↔ H4', H4' ↔ H5'/H5'', T(H6) ↔ T(CH_3) connectivities are indicated by boxed regions marked *a*–*f* respectively. The experimental conditions are the same as those in the Fig. 1 legend

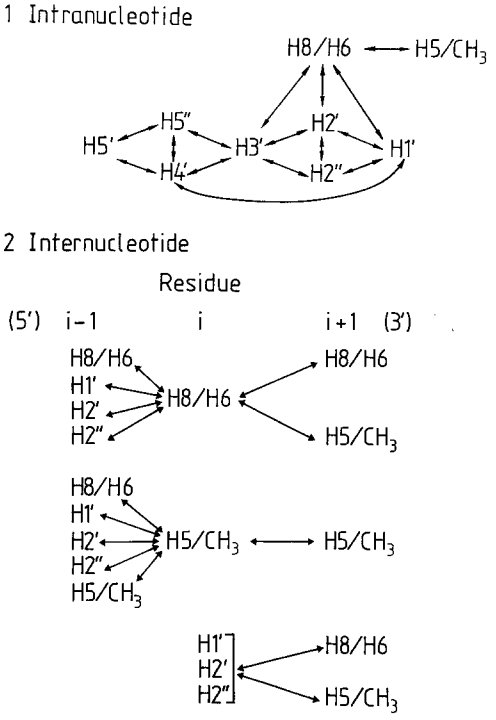

Fig. 3. Schematic illustration of the intra- and internucleotide interproton distances with values of $\lesssim 5$ Å in right-handed DNA which form the basis of the sequential resonance assignment procedure by means of NOE measurements. The distance relationships are applicable to both B- and A-DNA (Arnott and Hukins 1972; Clore and Gronenborn 1983; Gronenborn et al. 1984)

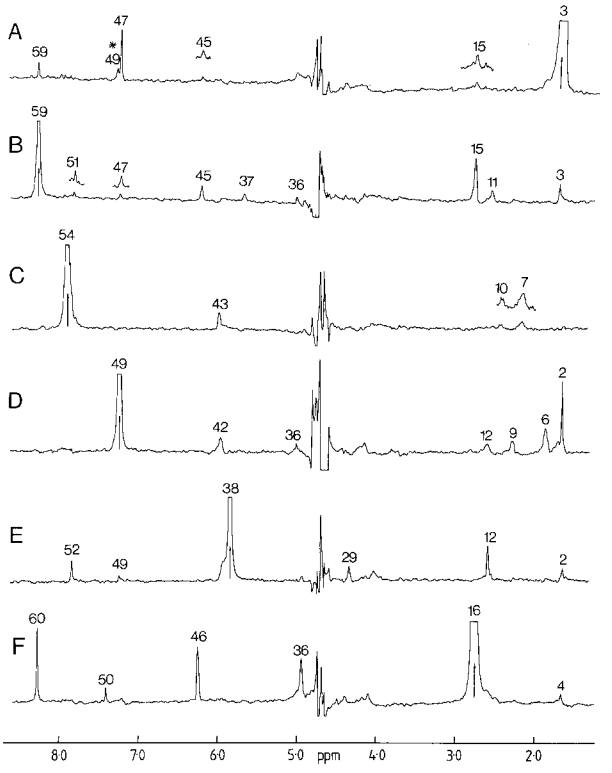

Fig. 4A–F. 500 MHz pre-steady state NOE difference spectra (off-resonance minus on-resonance irradiation) on the single-stranded 11-mer following irradiation of: **A** the $T_9(CH_3)$ resonance 3, **B** the A_8(H8) resonance 59, **C** the A_1(H8) resonance 54, **D** the T_4(H6) resonance 49, **E** the G_3(H1′) resonance 38, and **F** the A_{10}(H2′/H2″) resonance 16. The assignments of the other peaks seen in the difference spectra are given in Table 1. Note that a decrease in intensity of a particular resonance is seen as a positive peak in the difference spectrum. In **A**, the peak marked with a * is due to an NOE from peak 2 whose magnetization has been slightly perturbed by the tail of the selective irradiation pulse centred on peak 3 (note that peaks 2 and 3 are separated by only 8 Hz). The irradiating pulse was applied for 1 s for all NOE difference spectra and prior to Fourier transformation the difference free induction decays were multiplied by an exponential equivalent to a line broadening of 4 Hz. 800 transients were average for each difference spectrum. The experimental conditions are the same as those in the Fig. 1 legend

assignment of all non-exchangeable proton resonances (with the exception of the A(H2) protons which are not part of the cross-relaxation network) in right-handed single and double-stranded DNA helices. The initial deduction of an approximately right-handed helical conformation for the 11-mer is based on assignment of resonances by means of NOE measurements and is followed by refinement of the structure on the basis of the NOE data. Additional information derives from the demands and constraints presented by the J connectivities established from the COSY experiment, the known sequence of the 11-mer, the nature of the terminal residues, and the directionality of some of the internucleotide NOEs. As a result, the assignments are unambiguous and the structural information deduced is reliable.

Systematic pre-steady state NOE measurements were carried out by irradiating all the numbered resonances in Fig. 1 in turn. The selective irradiation pulse was applied for 1 s and control experiments; using different irradiation times for a few selected resonances indicated that the initial rate approximation was valid under these conditions. All NOE effects were reciprocal. Some examples of pre-steady state NOE difference spectra are shown in Fig. 4. The resonance assignments are given in Table 1, the complete set of NOEs is presented in Table 2, and a summary of the observed internucleotide NOEs is shown in Fig. 5. The interpretation of the complete NOE data set was thoroughly checked for self-consistency, as this stringent requirement provides an easy and reliable check for possible assignment errors (Reid et al. 1983a, b; Clore and Gronenborn 1983, 1984; Gronenborn et al. 1984; Weiss et al. 1984).

The solution structure of the single stranded 11-mer

Because the magnitude of the pre-steady state NOE is proportional to r^{-6}, the relative magnitudes of the

Table 1. Resonance assignments for the single-stranded DNA 11-mer determined by NOE measurements and homonuclear J-correlated spectroscopy. Chemical shifts (ppm from DSS) are at 30° C. The A(H2) protons resonate at 7.97 ppm (peak 57), 7.95 ppm (peak 56), 7.92 ppm (peak 55), and 7.85 ppm (peak 52) but have not been assigned to the individual adenine residues. This is because the A(H2) are $\gtrsim 5$ Å from the other non-exchangeable protons and hence are not part of the cross-relaxation network used in the NOE assignment procedure (see Fig. 3)

Residue	Chemical shift (ppm) of protons (peak No.)									
	H8	H6	CH_3	H1′	H2′	H2″	H3′	H4′	H5′	H5″
A_1	7.91 (54)			5.99 (43)	2.16 (7)	2.41 (10)	4.77 (34)	4.18 (26)	3.69 (17)	3.69 (17)
A_2	8.10 (58)			5.94 (40)	2.56 (12)	2.59 (13)	4.95 (36)	4.35 (30)		
G_3	7.85 (52)			5.85 (38)	2.56 (12)	2.56 (12)	4.95 (36)	4.32 (29)	4.18 (26)	4.12 (25)
T_4		7.26 (49)	1.63 (2)	5.97 (42)	1.83 (6)	2.25 (9)	4.73 (33)	4.04 (21)		
G_5	7.87 (53)			5.95 (41)	2.59 (13)	2.68 (14)	4.88 (35)	4.30 (28)	4.05 (22)	4.05 (22)
T_6		7.23 (48)	1.60 (1)	5.94 (40)	1.78 (5)	2.16 (7)	4.73 (33)	4.12 (25)		
G_7	7.80 (51)			5.65 (37)	2.49 (11)	2.49 (11)	4.88 (35)	4.24 (27)	4.00 (20)	3.94 (19)
A_8	8.25 (59)			6.18 (45)	2.71 (15)	2.71 (15)	4.95 (36)	4.35 (30)		
T_9		7.22 (47)	1.65 (3)	5.90 (39)	1.83 (6)	2.22 (8)	4.77 (34)	4.18 (26)		
A_{10}	8.29 (60)			6.27 (46)	2.76 (16)	2.76 (16)	4.95 (36)	4.38 (31)	4.12 (25)	4.10 (24)
T_{11}		7.43 (50)	1.67 (4)	6.11 (44)	2.25 (9)	2.25 (9)	4.52 (32)	4.07 (23)		

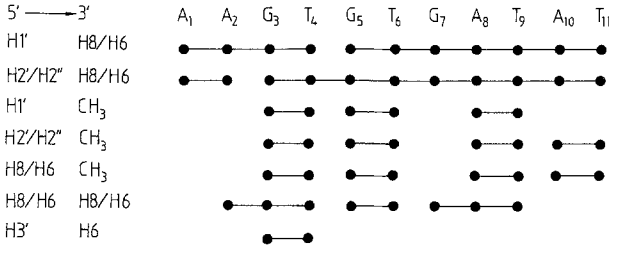

Fig. 5. Diagrammatic summary of the observed internucleotide NOEs for the single-stranded DNA 11-mer

NOEs (see Table 2) provide a sensitive probe with which to obtain a qualitative picture of the solution structure of the single-stranded 11-mer. In view of the much greater inherent flexibility of single-stranded DNA oligonucleotides relative to their double-stranded counterparts, no attempt has been made to calculate interproton distances from the NOE data using the NOEs arising from protons a known fixed distance apart as internal standards.

Considering the intranucleotide NOEs first, we note that with the exception of residues A_1 and G_5, $N_{H2'-H8/H6} \gg N_{H1'-H8/H6} \gtrsim N_{H3'-H8/H6}$ for the sugar-base NOEs and $N_{H1'-H2''} > N_{H1'-H2'} \sim N_{H1'-H4'}$ for the intra-sugar NOEs (see for example Fig. 4B, D–F). This pattern of NOEs is indicative of an *anti*-conformation about the glycosidic bond within the range $\chi \sim -115 \pm 30°$ and a deoxyribose conformation in the C1′-exo to C2′-endo range (Clore and Gronenborn 1983, 1984), characteristic of B-DNA (Arnott and Hukins 1972; Dickerson and Drew 1981). In A-DNA, the conformation about the glycosidic bond in low *anti* ($\chi \sim -154°$) and the sugar pucker 3′-endo (Arnott and Hukins 1972; Conner et al. 1982; Shakked et al. 1983) so that large intranucleotide NOEs would be observed between the H8/H6 and H3′ protons and small ones between the H8/H6 and H2′ protons. In the case of G_5, the sugar-base NOEs between the H1′, H2′, and H2″ sugar protons and the H8 base proton are approximately equal and much larger than the NOE between the H3′ and H8 protons. This is consistent either with a mixture of *syn* and *anti* conformations or with a low *syn* conformation with χ in the range $-20 \pm 15°$. In the case of residue A_1, $N_{H1'-H8} > N_{H2'-H8} > N_{H2''-H8} \gg N_{H3'-H8}$ (see Fig. 4C) which is consistent with a *syn* conformation with $\chi \sim 60 \pm 20°$. The sugar pucker conformation of residues A_1 and G_5, as judged by the intra-sugar NOEs involving the H1′, H2′, H2″, and H4′ protons also lie in the C1′-exo to C2′-endorange.

The sugar pucker can also be ascertained from the $J_{1'2'}$ coupling constant from the approximate empiricial relationship $\%[2'\text{-endo}] \sim 10J_{1'2'}$ (Lee and Tinoco 1980; Cheng et al. 1982). Because of the resonance overlap, we can only resolve $J_{1'2'}$ for eight out of the 11 residues, namely A_1 (9.3 Hz), G_3 (8.7 Hz), T_4 (9.0 Hz), G_7 (7.3 Hz), A_8 (7.1 Hz), T_9 (8.6 Hz), A_{10} (6.9 Hz), and T_{11} (6.9 Hz). Thus the degree of 2′-endo conformational purity lies in the range 69%–93%.

With the exception of the NOEs involving the H8/H6 protons of adjacent residues, all the internucleotide NOEs exhibit directional specificty (see Fig. 5). In particular, internucleotide NOEs are observed between the methyl protons of the T residues and the H8/H6 proton of the adjacent 5′ residue but not of the adjacent 3′ residue (see, for example, Fig. 4A). Similarly, internucleotide NOEs are observed between the H1′, H2′, and H2″ sugar protons of a given residue and the H8/H6 and methyl protons of the adjacent 3′ residue but not of the

Table 2. Magnitudes of the pre-steady state NOEs (irradiation time 1 s) observed for the single-stranded DNA 11-mer. The experimental conditions are the same as those in the Fig. 1 legend

A. Intranucleotide NOEs

Proton Pair	NOE (%)										
	A_1	A_2	G_3	T_4	G_5	T_6	G_7	A_8	T_9	A_{10}	T_{11}
Intra-sugar											
H1′-H2′	− 2	−3	} −14	− 4	[a]	− 3	} −15	} −16	− 3	} −11	} −8
H1′-H2″	− 8	[a]		− 8	− 7	− 9			− 9		
H1′-H4′	− 1	−3	− 3	− 2	− 4	− 2	− 2	− 2	− 2	− 2	−1
H2′-H2″	−10	[d]	[c]	[e]	−15	−15	[c]	[c]	[e]	[c]	[c]
H2′-H3′	− 4	[b]	[b]	[f]	− 6	[f]	} −21	} −20	− 7	} −10	} −7
H2″-H3′	− 3	−2	[b]	− 3	− 4	− 1			− 4		
H3′-H4′	[h]	[g]	− 5	− 4	− 5	− 4	− 6	[g]	[h]	− 3	−1
Sugar-base											
H1′-H8/H6	− 5	−3	− 4	− 2	− 7	− 2	− 7	− 3	− 3	− 2	−1
H2′-H8/H6	− 3	−8	} −14	−11	− 6	−11	} −23	} −20	−11	} −12	} −4
H2″-H8/H6	− 1	−2		− 3	− 6	− 3			− 2		
H3′-H8/H6	≲ − 0.5	−1	− 1	− 1	− 1	− 0.5	− 2	− 1	− 2	− 1	−1
Intra-base											
H6-CH_3				−10		−10			− 9		−4

B. Internucleotide NOEs

Proton of 5′nucleotide	Proton of 3′nucleotide	NOE (%)									
		A_1pA_2	A_2pG_3	G_3pT_4	T_4pG_5	G_5pT_6	T_6pG_7	G_7pA_8	A_8pT_9	T_9pA_{10}	$A_{10}pT_{11}$
H1′	H8/H6	−0.5	−2	−1		−1	−1	−2	−0.5	−0.5	−0.5
H1′	CH_3			−3		−2			−1		−1
H2′	H8/H6	−1		} −6	−1	−3	−1	} −5	} −6	−1	} −3
H2″	H8/H6	−2			−2	−3	−1			−1	
H2′	CH_3			} −2		−1			} −2		} −1
H2″	CH_3					−1					
H8/H6	H8/H6		−1	−0.5		−0.5		−0.5	−0.5		
H8/H6	CH_3			−3		−3			−3		−2
H3′	H6			−0.5							

[a] A NOE of −17% is observed between peak 13 [G_5(H2′) and A_2(H2″)] and peaks 41 [G_5(H1′)] and 40 [A_2(H1′)] but cannot be resolved owing to the very close proximity (~ 6 Hz) and relatively large line widths of peaks 41 and 40

[b] A NOE of −26% is observed between peak 12 [A_2(H2′), G_3(H2′), and G_3(H2″)] and peak 36 [A_2(H3′) and G_3(H3′)]

[c] The H2′ and H2″ resonances of G_3 (peak 12), G_7 (peak 11), A_8 (peak 15), A_{10} (peak 16), and T_{11} (peak 9) are superimposed

[d] The NOE between the H2′ (peak 12) and the H2″ (peak 13) resonances of A_2 cannot be quantitated as they are separated by only 13 Hz and their line widths are broad

[e] A NOE of −30% is observed between peak 6 [T_4(H2′) and T_9(H2″)] and peaks 8 [T_9(H2″)] and 9 [T_4(H2″)] but cannot be resolved owing to the close proximity (~ 15 Hz) and large line widths of peaks 8 and 9

[f] A NOE of −9% is observed between peak 33 [T_4(H3′) and T_6(H3′)] and peaks 5 [T_4(H2′)] and 6 [T_4(H2″)] but cannot be resolved owing to the close proximity (~ 20 Hz) and large line widths of peaks 5 and 6

[g] A NOE of −10% is observed between peak 36 [A_2(H3′) and A_8(H3′)] and peak 30 [A_2(H4′) and A_8(H4′)]

[h] A NOE of −8% is observed between peak 34 [A_1(H3′) and T_9(H3′)] and peak 26 [A_1(H4′) and T_9(H4′)]

adjacent 5′ residue (see for example Fig. 4A, B, D−F). This pattern of internucleotide NOEs is only compatible with a right-handed helical structure in which the bases are stacked (Reid et al. 1983a; Feigon et al. 1982; Clore and Gronenborn 1983, 1984; Gronenborn et al. 1984). In addition, the internucleotide NOEs between the H2′ and H2″ protons and the H8/H6 proton of the adjacent 3′-residue are smaller than the intranucleotide NOEs between the H2′ and H8/H6 protons. This confirms the overall B-type geometry, as in the A conformation the internucleotide distance between the H2′ proton and the H8/H6 proton of the adjacent 3′-residue is much shorter than the intranucleotide H2′-H8/H6 distance (Reid et al. 1983a, b; Clore and Gronenborn 1983, 1984). Finally, the extensive stacking of the bases is confirmed by the observation of internucleotide NOEs between the H8/H6 protons of adjacent residues.

Concluding remarks

In the present paper we have demonstrated the combined power of one-dimensional pre-steady state NOE measurements and two-dimensional homonuclear J-correlated spectroscopy in obtaining virtually complete resonance assignments for a relatively long single-stranded DNA oligonucleotide, namely an 11-mer. The relative magnitudes of the NOEs are readily interpretable in a qualitative manner to yield low resolution structural information. In the case of the 11-mer, the NOE data are indicative of an overall right-handed B-type conformation with extensive base stacking. It therefore seems likely that most of the favourable enthalpy driving helix formation in DNA can be attributed to base stacking interactions given that inter-residue hydrogen bonding interactions are not available in single-stranded DNA. A similar conclusion has been reached on the basis of thermodynamic studies of the helix-coil transition (Turner et al. 1981). Within the overall B-type structure, there is quite a large degree of variability, as illustrated, for example, by the variation in sugar pucker within the C1′-exo to C2′-endo range and the departure from the anti-conformation about the glycosidic bond for residues A_1 *(syn)* and G_5 (low *syn* or a *syn/anti* mixture). In this respect it is interesting to note that a previous NOE study on the single-stranded DNA tetramer 5′d ATGT showed that the first residue dAp was in the *syn* conformation and the dG residue existed as a *syn/anti* mixture (Neumann et al. 1982). Thus, the *syn* conformation may represent an intrinsic conformational preference of the first dAp residue, and indeed is the preferred conformation of 3′AMP (Ap) (Gueron et al. 1973). Similarly, the *syn/anti* mixture may be a characteristic of a dG residue flanked by a dT residue on its 5′ and 3′ sides.

Finally, it should be pointed out that although single-stranded DNA is obviously more flexible than double-stranded DNA, the single-stranded DNA 11-mer definitely possesses substantial order in solution under the experimental conditions employed. This is further supported by optical melting studies which indicate that the 11-mer melts in a cooperative manner (Tm ~ 36° C) and that at 30° C less than 20% of the 11-mer is in a disordered state (unpublished data). The local structural variations are most likely influenced by base sequence and the overall structure of the single strand is similar to the structure adopted by an individual single strand in double-stranded B-DNA. Thus the single helical structure is potentially able to adopt a double helical structure with minimal conformational adjustments. It is also important to bear in mind that the NOE data do not permit one to define a unique structure fo the single-stranded 11-mer in solution since NOE data, although of high quality, are limited to very close-range (< 5 Å) ordered structures. Indeed, the data are entirely compatible with a conformational equilibrium between different but closely related species within the constraints of an overall right-handed B-DNA helical geometry.

Acknowledgements. This work was supported by the Medical Research Council (GMC and AMG) and the Lister Institute of Preventive Medicine (GMC). GMC is a Lister Institute Research Fellow. The NMR spectra were recorded on the AM500 spectrometer of the Medical Research Council Biomedical NMR Centre at the National Institute for Medical Research.

References

Altona C (1982) Conformational analysis of nucleic acids: determination of backbone geometry of single-helical RNA and DNA in aqueous solution. Rec J R Netherlands Chem Soc. 101: 413–433

Arnott S, Hukins DWL (1972) Optimized parameters for A-DNA and B-DNA. Biochem Biophys Res Commun 47: 1504–1509

Arnott S, Chandrasekaran R, Hall IH, Puigjaner LC, Walker JK, Wang M (1983) DNA secondary structures: helices, wrinkles and junctions. Cold Spring Harbor Symp Quant Biol 47: 53–65

Aue WP, Bartholdi E, Ernst RR (1976) Two dimensional spectroscopy: application to nuclear magnetic resonance. J Chem Phys 64: 2229–2246

Baumann R, Wider G, Ernst RR, Wüthrich K (1981) Improvement of 2D NOE and 2D correlated spectra by symmetrization. J Magn Reson 44: 402–406

Camerman N, Fawcett JK, Camerman A (1976) Molecular structure of a deoxyribose-dinucleotide, sodium thymidylyl-(5′→3′)-thymydylate-(5′) hydrate (pTpT), and a possible structural model for polythymiydilate. J Mol Biol 107: 601–621

Cheng DM, Sarma RH (1977) Intimate details of the conformational characteristics of deoxyribodinucleoside monophosphates in aqueous solution. J Am Chem Soc 99: 7333–7348

Cheng DM, Kan LS, Leutzinger EE, Jayaraman K, Miller PS, Ts'o POP (1982) Conformational study of two short pentadeoxyribonucleotides, d-CpCpApApG and d-CpTpTpGpG, and their fragments by proton nuclear magnetic resonance. Biochemistry 21: 621–630

Clore GM, Gronenborn AM (1983) Sequence-dependent structural variations in two right handed alternating pyrimidine-purine DNA oligomers in solution determined by nuclear Overhauser enhancement measurements. EMBO J 2: 2109–2115

Clore GM, Gronenborn AM (1984) A nuclear Overhauser enhancement study of the solution structure of a double stranded DNA undecamer comprising a portion of the specific target site for the cyclic AMP receptor protein in the *gal* operon: sequential resonance assignment. Eur J Biochem 141: 119–129

Clore GM, Gronenborn AM, McLaughlin LW (1984) The structure of the ribotrinucleoside diphosphate codon UpUpC bound to $tRNA^{Phe}$ from yeast: a time dependent transferred nuclear Overhauser enhancement study. J Mol Biol 174: 163–173

Conner BN, Takano T, Tanaka S, Itakura K, Dickerson RE (1982) The molecular structure of d(CpCpGpG), a fragment of right handed double helical A DNA. Nature 215: 294–299

Dickerson RE, Drew HR (1981) Structure of a B-DNA dodecamer. J Mol Biol 149: 761–786

Dickerson RE, Drew HR, Conner BN, Kopka ML, Pjura PE (1983) Helix geometry and hydration in A-DNA, B-DNA and Z-DNA. Cold Spring Harbor Symp Quant Biol 47: 13–24

Dobson CM, Olejniczak ET, Poulsen FM, Ratcliffe RG (1982) Time development of proton nuclear Overhauser effects in proteins. J Magn Reson 48: 97–110

Feigon J, Wright JM, Leupin W, Denny WA, Kearns DR (1982) Use of two-dimensional NMR in the study of a double stranded DNA decamer. J Am Chem Soc 104: 5540–5541

Gait MJ, Matthes HWD, Singh M, Sproat BS, Titmas RC (1982) Synthesis of oligodeoxyribonucleotides by a continuous flow phosphotriester method on a kieselguhr/polyamide support. In: Gassen HG, Lang A (eds) Chemical and enzymatic gene synthesis. Verlag Chemie, Weinheim, pp 1–42

Gronenborn AM, Clore GM, Jones MB, Jirizny J (1983) A nuclear Overhauser enhancement study on the imino proton resonances of a DNA pentadecamer comprising the specific target site of the cyclic AMP receptor protein in the *ara* BAD operon. FEBS Lett 165: 216–222

Gronenborn AM, Clore GM, Kimber BJ (1984) An investigation into the solution structures of two self-complementary DNA oligomers, 5′d(CGTACG) and 5′d(ACGCGCGT) by means of nuclear Overhauser enhancement measurements. Biochem J 221: 723–736

Guéron M, Chachaty C, Tran-Dinh S (1973) Properties of purine nucleotides studied by the Overhauser effect: conformations, flexibility and aggregation. Ann NY Acad Sci 222: 307–323

Hare DR, Wemmer DE, Chou SH, Drobny G, Reid BR (1983) Assignment of the non-exchangeable proton resonances of d(CGCGAATTCGCG) using two-dimensional nuclear magnetic resonance methods. J Mol Biol 171: 319–336

Karplus M (1963) Vicinal proton coupling in nuclear magnetic resonance. J Am Chem Soc 85: 2870–2871

Kornberg A (1980) DNA replication. Freeman, San Francisco

Kowalczykowski SC, Bear DG, von Hippel PH (1981) Single-stranded DNA binding proteins. In: Boyer PD (ed) The enzymes: nucleic acids, Part A, vol 14. Academic Press, New York, pp 373–444

Lee CH, Tinoco I (1980) Conformation studies of 13 trinucleoside diphosphate by 360 MHz PMR spectroscopy: a bulged base conformation. I. Base protons and H1′ protons. Biophys Chem 11: 283–294

Maxam AM, Gilbert W (1980) Sequencing end-labelled DNA with base-specific chemical cleavages. Methods Enzymol 65: 499–560

McEntee V, Weinstock GM, Lehman IR (1981) DNA and nucleoside triphosphate binding properties of rec A protein from Escherichia coli. Prog Nucl Acid Res Mol Biol 26: 265–279

Mellema JR, Haasnoot CAG, Boom JH van, Altona C (1981) Complete assignment and conformational analysis of a deoxyribotetranucleotide, d(TAAT): a 360 and 500 MHz NMR study. Biochim Biophys Acta 655: 256–264

Meselson M (1967) The molecular basis of genetic recombination. In: Brink A (ed) Heritage from Mendel. The University of Wisconsin Press, pp 81–104

Neumann JM, Huynh-Dinh T, Kan SK, Genisul B, Ingolen J, Tran-Dinh S (1982) DNA fragment conformations: ^{1}H-NMR and relaxation studies of 2′-deoxyadenylyl(3′-5′)thymidylyl-(3′5′)deoxyguanosylyl(3′5′)thymidine, d(ATGT), in neutral aqueous solution. Eur J Biochem 121: 317–323

Noggle J, Schirmer RE (1971) The nuclear Overhauser effect – chemical applications. Academic Press, New York

Olsthoorn CSM, Bostelaar LJ, van Boom JH, Altona C (1980) Conformational characteristics of the trinucleoside diphosphate dApdApdA and its constituents from nuclear magnetic resonance and circular dichroism studies. Eur J Biochem 112: 95–110

Poulsen FM, Hoch JC, Dobson CM (1980) A structural study of the hydrophobic box region of lysosyme in solution using nuclear Overhauser effects. Biochemistry 19: 2597

Radding CM (1978) Genetic recombination: strand transfer and mismatch repair. Annu Rev Biochem 47: 847–880

Redfield AG, Gupta RK (1971) Pulsed NMR study of the structure of cytochrome c. Cold Spring Harbor Symp Quant Biol 36: 405–419

Reid DG, Salisbury SA, Bellard S, Shakked Z, Williams DH (1983a) Proton nuclear Overhauser effect study of the structure of a deoxyoligonucleotide duplex in aqueous solution. Biochemistry 22: 2019–2025

Reid DG, Salisbury SA, Brown T, Williams DH, Vasseur JJ, Rayner B, Imbach JL (1983b) Use of inter-proton nuclear Overhauser effects to assign the nuclear magnetic resonance spectra of oligodeoxynucleotide and hybrid duplexes in aqueous solution. Eur J Biochem 135: 307–314

Rich A (1983) Right handed and left handed DNA: conformational information in genetic material. Cold Spring Harbor Symp Quant Biol 47: 1–12

Scheek RM, Russo N, Boelens R, Kaptein R, Boom JH van (1983) Sequential resonance assignments in DNA ^{1}H-NMR spectra by two dimensional NOE spectroscopy. J Am Chem Soc 105: 2914–2916

Shakked Z, Rabinovich D, Kennard O, Cruze WBT, Salisbury SA, Viswamitra MA (1983) Sequence dependent conformation of an A-DNA double helix: the crystal structure of the octamer d(GGTATACC). J Mol Biol 166: 183–201

Turner DH, Petersheim N, De Poisco Albergo D, Dewey TG, Freier SM (1981) Why do nucleic acids form helices? In: Sarma RH (ed) Biomolecular Stereodynamics, vol 1. Adenine Press, New York, pp 429–438

Viswamitra MA (1983) Structural diversity in DNA: from monomer structures to oligonucleotides. Cold Spring Harbor Symp Quant Biol 47: 25–31

Wagner G, Wüthrich K (1979) Truncated driven nuclear Overhauser effect (TOE): a new technique for studies of selective ^{1}H-^{1}H Overhauser effects in the presence of spin diffusion. J Magn Reson 33: 675–680

Wagner G, Wüthrich K (1982) Sequential resonance assignments in protein ^{1}H-nuclear magnetic resonance spectra: basic pancreatic trypsin inhibitor. J Mol Biol 155: 347–366

Wagner G, Kumar A, Wüthrich K (1981) Systematic application of two-dimensional ^{1}H-nuclear magnetic resonance techniques for studies of proteins: 2. Combined use of correlated spectroscopy and nuclear Overhauser spectroscopy for sequential assignments of backbone resonances and elucidation of polypeptide secondary structures. Eur J Biochem 114: 375–384

Wang AHJ, Fujii S, Boom JH van, Rich A (1983) Right-handed and left-handed double helical DNA: structural studies. Cold Spring Harbor Symp Quant Biol 47: 33–44

Weiss MA, Patel DJ, Sauer RT, Karplus M (1984) Two-dimensional ^{1}H-NMR study of the λ operator site 0_L1: a sequential assignment strategy and its application. Proc Natl Acad Sci USA 81: 130–134

Wider G, Lee KH, Wüthrich K (1982) Sequential resonance assignment in protein ^{1}H-nuclear magnetic resonance spectra: glucagon bound to perdeuterated dodecylphosphocholine micelles. J Mol Biol 155: 367–388

Wider G, Macura S, Kumar A, Ernst RR, Wüthrich K (1984) Homonuclear two-dimensional ^{1}H-NMR of proteins: experimental procedures. J Magn Reson 56: 207–234